



Effect of Nickel Coating on the Interfacial Shear Strengths of SiC Fiber Reinforced 7075 Aluminum Composites

Liang-Guang Chen and Su-Jien Lin^{*z}

Department of Materials Science and Engineering, National Tsing-Hua University, Hsinchu, Taiwan

The effect of electroless nickel coating on the interfacial shear strengths of silicon carbide continuous fiber reinforced AA 7075 aluminum matrix composites (SiC_f/7075Al) was investigated using a push-out method with a tungsten carbide (WC) cone indenter. During indentation, no rupture of fibers was observed. This showed that the push-out test can measure the interfacial shear strength of SiC_f/7075Al precisely. The 160 MPa interfacial shear strength of the specimen without coating decreases to 120 MPa for the specimen with 0.5 μm nickel coating, even to 20 MPa with 0.8 μm nickel coating, and then slightly increases with increasing coating film thickness. Nickel film reacted with aluminum matrix to form porous nickel aluminide intermetallic compounds during processing and to lower the interfacial shear strength.

© 2002 The Electrochemical Society. [DOI: 10.1149/1.1485082] All rights reserved.

Manuscript submitted June 4, 2001; revised manuscript received February 2, 2002. Available electronically June 12, 2002.

Research on new materials with high strength, high stiffness, high fracture toughness, low densities, high thermal conductivity, and low coefficients of thermal expansion (CTEs) for application in aerospace and electronic packaging industries are of tremendous interest to materials scientists at present. Among these new materials, metal matrix composites reinforced by continuous fibers of high strength, high stiffness, and good thermal stability have been considered as potential candidates.¹ Since the 1960s, continuous fiber reinforced metal matrix composites have been developed quickly, and the most successful, reliable processing method for them is diffusion bonding. Because the interfacial shear strengths between fibers and matrices seriously affect the tensile strengths and fracture toughness of composites,^{2,3} research on the interfacial shear strength has attracted much more attention.⁴⁻⁸ The three most used methods for the measurement of interfacial shear strength have been developed as follows⁹

1. Pull out: A part of the fiber is embedded into matrix. The exposed part is clamped, and then the fiber is pulled out. The applied loads for pulled-out fibers are measured, and the interfacial shear strengths can be obtained. This method is not suitable for metal matrix composites because of the difficulty of specimen preparation.

2. Push out: Composite specimens are sliced to several hundred micrometers thick perpendicular to fibers. Fibers are pushed out using an indenter, and stress-strain curves are measured to calculate the interfacial shear strength. This method is suitable for most ceramic fiber reinforced metal matrix composites.

3. Fragmentation: Composite specimens are tensile tested, followed by matrix etching and fiber extracting. The average length of fragmented fibers is measured to calculate the interfacial shear strength. This method is also suitable for most ceramic fiber reinforced metal matrix composites, but the elongation of the matrix must be greatly larger than that of fibers using this method.

In this research, fiber push-out was used to measure the interfacial shear strengths of continuous fiber reinforced metal matrix composites according to the following advantages⁹: (i) stress-displacement curves can be obtained easily, (ii) more data can be obtained in a same specimen for a more precise result, and (iii) the sensitivity to interfacial conditions is high. The typical stress-displacement curve of a fiber push-out test can be divided into three steps

1. Elastic deformation: the linear region in the curve at first.
2. Interfacial debonding: the region when the stress drastically drops. It occurs when the applied stress is larger than the interfacial shear strength. The maximum stress indicates the interfacial shear strength.
3. Interfacial friction sliding: after interfacial debonding, the fiber

slides, and the stress gradually decreases. The stresses after the maximum value mean the interfacial friction forces, which decrease with increasing displacement of fibers due to the decreasing contact area.

Silicon carbide fibers were electrolessly nickel coated previously to investigate the effect of different interfacial treatments on the interfacial shear strengths of SiC_f/7075Al composites.

Experimental

Materials.—Continuous SiC fibers (SCS-8) from Textron Corp. with a diam of 142 μm were used as reinforcements. The SiC fibers have a high strength (4000 MPa), a high elastic modulus (380 GPa), a low density (3.2×10^3 kg/m³), high thermal conductivity (270 W/mK), and a low CTE (5×10^{-6} 1/K).¹⁰ Hence, the mechanical properties of SiC fiber reinforced composites are expected to be very good.

Commercial AA 7075 aluminum alloy plates with a thickness of 1.5 mm were used as the matrix.

Electroless nickel plating.—Fiber surfaces were treated prior to electroless nickel plating by surface cleaning, sensitization, and activation in order to achieve good nickel coated films. For surface cleaning, the fibers were immersed in acetone and HNO_{3(aq)} under ultrasonic vibration and continuous stirring for 15 min. They were subsequently sensitized in an aqueous solution containing stannous chloride (SnCl₂·H₂O, 10 g/L) and hydrochloric acid (HCl, 40 mL/L) for 15 min, and then activated in an aqueous solution containing palladium chloride (PdCl₂, 0.25 g/L) and HCl (2.5 mL/L) for another 15 min. The activated fibers were finally washed by deionized water and baked at 80°C.

Electroless nickel plating solution was prepared by adding the components in the following order

1. NiCl ₂ ·6H ₂ O	30 g/L
2. NaOOCCH ₂ CH ₂ COONa·6H ₂ O	10 g/L
3. H ₂ NCH ₂ COOH	10 g/L
4. NaH ₂ PO ₂ ·H ₂ O	20 g/L
5. Pb(NO ₃) ₂	2.5 mg/L

Plating was performed at 80°C under ultrasonic vibration for 5, 10, 20, and 40 min to obtain different thicknesses of nickel films.

Preparation of composite specimens.—Alternate layers of 1 mm spaced nickel coated fibers and AA 7075 aluminum alloy plates of 1.5 mm in thickness were stacked and diffusion bonded at 465°C, 45 MPa in a vacuum of 10⁻² Torr for 30 min to obtain SiC_f(Ni)/7075Al composites. The consolidated composite specimens were then solid-solution treated at 470°C for 1 h, water quenched to room temperature, and then T6 treated in an oil bath at 120°C for 24 h.

* Electrochemical Society Active Member.

^z E-mail: sjlin@mse.nthu.edu.tw

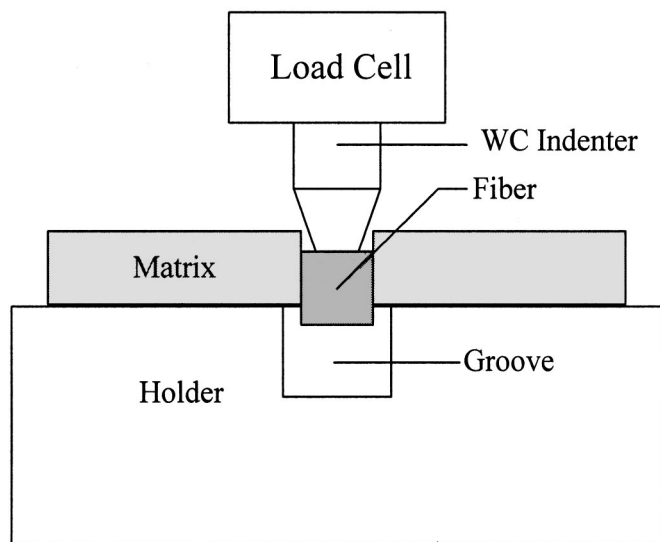


Figure 1. Experimental setup for the fiber push-out test.

Measurement of interfacial shear strength.—The T6 treated composite specimens were sliced to 1 mm thick perpendicular to fiber axis using a low speed diamond saw and then polished to 700 μm thick. The polished specimens were then placed on a steel holder with a groove of 300 μm in width and 5 mm in depth, as shown in Fig. 1. The SiC fiber to be indented was aligned to the center of the groove, and then the specimen was mounted onto the holder. The indentation was conducted using an Instron testing machine with a WC cone indenter with a cone angle of 30° and a plateau of 100 μm in diam on the tip.

The fibers were aligned to the cone tip and then indented at a rate of 10 $\mu\text{m}/\text{min}$. From the stress-displacement curves, the interfacial shear strengths of $\text{SiC}_f/7075\text{Al}$ composites were obtained by the equation¹¹

$$\tau = \frac{P}{2\pi rt} \quad [1]$$

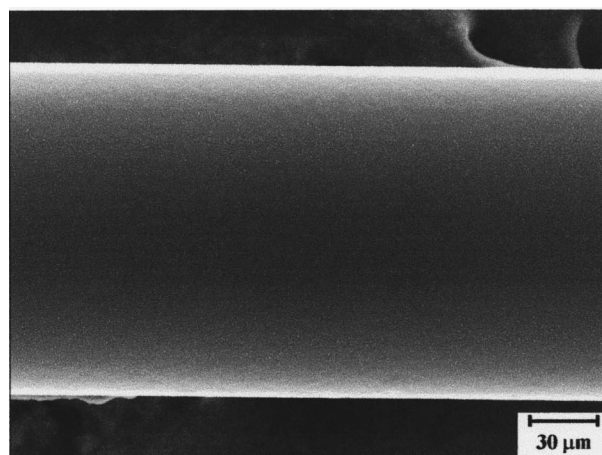
where τ , p , r , and t are the interfacial shear strength, maximum load, fiber radius, and specimen thickness, respectively.

In the measurement of the interfacial shear strengths of different fibers in the same composite, the data deviation was smaller than 5%, indicating good data reliability by fiber indentation. After push out, the fibers were pushed back to measure the interfacial shear strengths again for comparison.

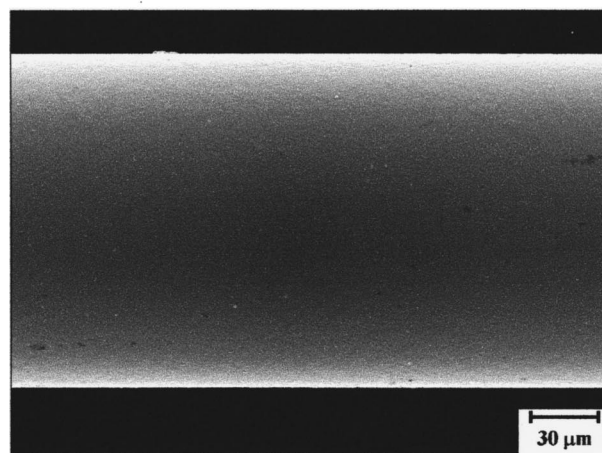
The surface morphologies of nickel coated fibers, the microstructures of composites, and the surface morphologies of the indented specimens were examined by a scanning electron microscope (SEM). The SEM backscattering electron image (BEI) and energy dispersion spectrum (EDS) were used to investigate the interfacial microstructures of the composites. The surface morphologies of the indented fibers and the surrounding matrix, which were obtained by tearing up the composites along the interface between two aluminum plates, were also examined by SEM.

Results and Discussion

Electroless nickel plating.—Figure 2 shows the SEM micrographs of the surface morphologies of SCS-8 SiC fibers before and after electroless nickel plating for 5 min. A continuous nickel film with few freely precipitated nickel particles was uniformly coated on the surface of fiber. All the surface morphologies of fibers after electroless nickel plating for 10, 20, and 40 min are the same as that



(a)



(b)

Figure 2. Surface morphologies of SCS-8 SiC fibers, (a) as-received and (b) after electroless nickel plating for 5 min.

for 5 min. Figure 3 shows that the thickness of coated nickel films increase linearly with increasing plating time at a deposition rate of 0.07 $\mu\text{m}/\text{min}$.

Microstructures of $\text{SiC}_f/7075\text{Al}$ composites.—Figures 4a and b show the microstructures of $\text{SiC}_f/7075\text{Al}$ composites containing fibers without nickel coating and with an nickel coating of 3.0 μm thick, respectively. It is well known that nickel reacts with aluminum to form intermetallic compounds at elevated temperatures.¹² Same interfacial reactions between electrolessly coated nickel films and aluminum matrix after diffusion bonding were also observed in this research. Figures 5a-d show the SEM micrographs of fiber/matrix interfaces in $\text{SiC}_f/7075\text{Al}$ composites containing nickel coated fibers with different film thicknesses. Obvious reactions occurring at the interfaces were found. According to SEM EDS analyses and an Al-Ni phase diagram,¹³ the nickel coated layer with a thickness of 0.5 μm reacted completely with the aluminum matrix and formed stoichiometry NiAl_3 intermetallic compound as shown in Fig. 5a. With increasing nickel film thickness, the nickel aluminate compounds tended to contain more nickel. With a nickel film thickness of 0.8 μm , mixed NiAl_3 and porous Ni_2Al_3 compounds formed as shown in Fig. 5b. As shown in Fig. 5c, with a nickel film thickness of 1.7 μm , the compounds NiAl_3 , Ni_2Al_3 , NiAl , and Ni_3Al existed, and also a part of the coated nickel film retained.

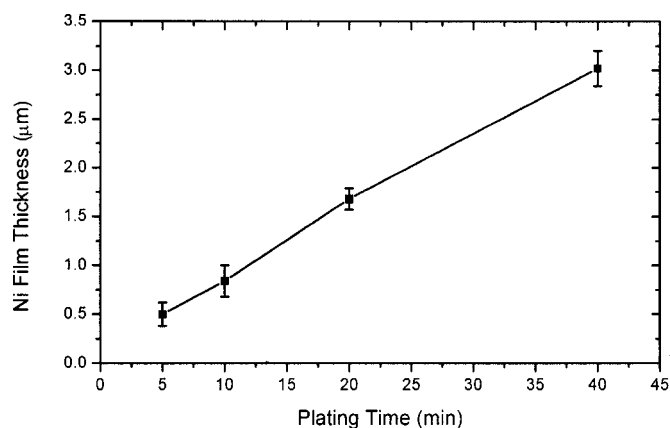


Figure 3. Relationship of film thickness of electroless nickel coating to plating time.

With increasing nickel film thickness to 3.0 μm , the fractions of NiAl and Ni₃Al increased, and the retained nickel film in the inner layer was obviously found.

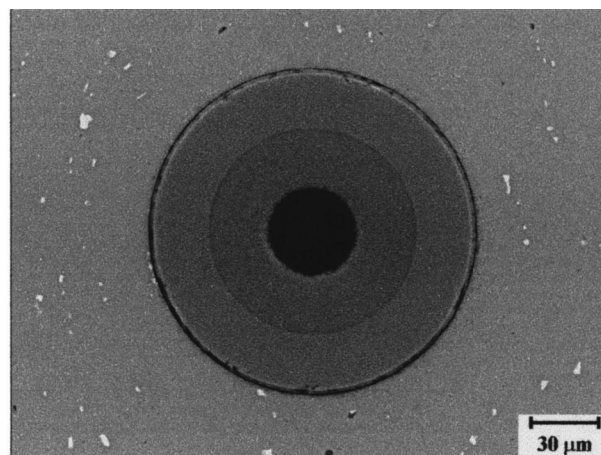
Effect of nickel coated film thickness on interfacial shear strength.—Figure 6 shows the interfacial shear strengths of composites reinforced by fibers without nickel coating and with nickel coatings of different film thicknesses in push-out tests. Without nickel coating, the composites exhibited the highest interfacial shear strength of 160 MPa, indicating strong interfacial bonds obtained at 465°C and 45 MPa in a vacuum of 10^{-2} Torr for 30 min. The interfacial shear strength of the composite reinforced by nickel coated fibers with a thickness of 0.5 μm decreased to 120 MPa and even lowered to 20 MPa with increasing nickel film thickness to 0.8 μm . As the thickness of the nickel coated films continued to increase, the interfacial shear strengths of composites slightly increased.

Figure 7 shows the surface morphology of indented SiC_f/7075Al composite containing fibers without electroless nickel coating. Fibers were pushed out without the deformation or fracture of both fibers and matrix, indicating that interfacial shear strength can be obtained precisely by fiber indentation. By tearing up the composite specimens, surface morphologies of the SiC fibers and the aluminum matrix before and after fiber push-out tests were obtained as shown in Fig. 8. Before fibers were pushed out, smooth fiber surfaces similar to as-received one and the matrix with some pores resulting from hot pressing were observed, as shown in Fig. 8a and b. No chemical reaction between the carbon rich layer on SCS-8 fiber surface and the aluminum matrix occurred even under hot pressing at 465°C which is near the solidus temperature of the 7075 aluminum alloy.

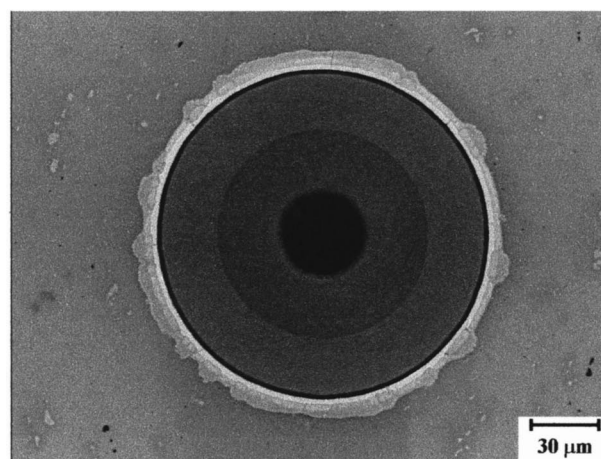
After fibers were pushed out, as shown in Fig. 8c and d, the 7075 aluminum alloy was found to adhere on the surface of SiC fiber, and obvious deformation of the matrix occurred due to the friction sliding of the fiber, both indicating a good physical bonding of the fiber and the matrix. A strong mechanical bonding, which resulted from the high pressure and high temperature of hot pressing and the large radial compression stresses provided by the aluminum matrix during cooling process of the composites, led to the highest interfacial shear strength and the obvious deformation of the matrix. The radial compression stress (σ_0) can be calculated using the equation¹⁴

$$\sigma_0 = \frac{E_m(\alpha_m - \alpha_f)\Delta T}{1 + \nu_m} \quad [2]$$

where E_m is the Young's modulus of the matrix, and α_m , α_f are the coefficients of thermal expansion of the matrix and the fiber, respectively. Poisson's ratio of the matrix is ν_m , and ΔT is the temperature difference during cooling where the thermal stresses build up. In



(a)



(b)

Figure 4. Microstructures of SiC_f/7075Al composites containing fibers (a) without and (b) with an electroless nickel coating 3.0 μm thick.

this research, $E_m = 71$ GPa, $\alpha_m = 25.2 \times 10^{-6}$ 1/K, $\alpha_f = 5 \times 10^{-6}$ 1/K, $\nu_m = 0.33$, and $\Delta T = (415^\circ\text{C} - RT)$. According to Eq. 2, σ_0 was obtained as 420 MPa. The high interfacial shear strength is proportional to the large compression stress by a factor of friction coefficient.

Figure 9 shows the surface morphologies of the matrices of torn up SiC_f/7075Al composites containing nickel coated fibers with different film thicknesses after indentation. Reactions between the nickel coated layers and the aluminum matrix were observed in all composites as also seen in Fig. 5. The formation of brittle intermetallic compounds led to the easy fracture of interfaces and fiber sliding, resulting in the reduction in interfacial shear strength as previously shown in Fig. 6. With the nickel film thickness of 0.5 μm , NiAl₃ intermetallic compound formed. Flat surfaces of indented fibers and matrix without the present of matrix deformation and friction sliding were observed as shown in Fig. 9a. With increasing nickel film thickness, porous Ni₂Al₃ compound formed and drastically lowered the interfacial shear strength as reported.¹⁵ Especially the composite containing fibers with a nickel film thickness of 0.8 μm exhibited the lowest interfacial shear strength of only 20 MPa due to the high content of porous Ni₂Al₃ compound as observed on the surface of indented matrix shown in Fig. 9b. With increasing nickel film thickness to 1.7 μm , less porous Ni₂Al₃ compound existed at interfaces as shown in Fig. 9c, and thus the inter-

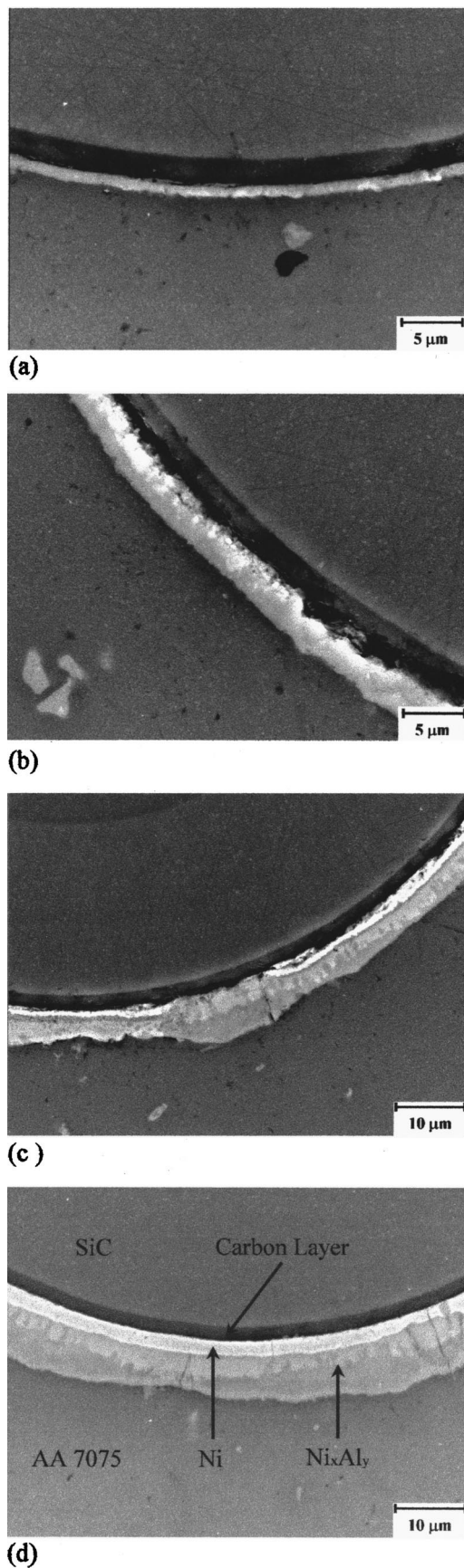


Figure 5. Microstructures of fiber/matrix interfaces in SiC_f/7075Al composites containing fibers with electroless nickel coating of (a) 0.5, (b) 0.8, (c) 1.7, and (d) 3.0 μm thick.

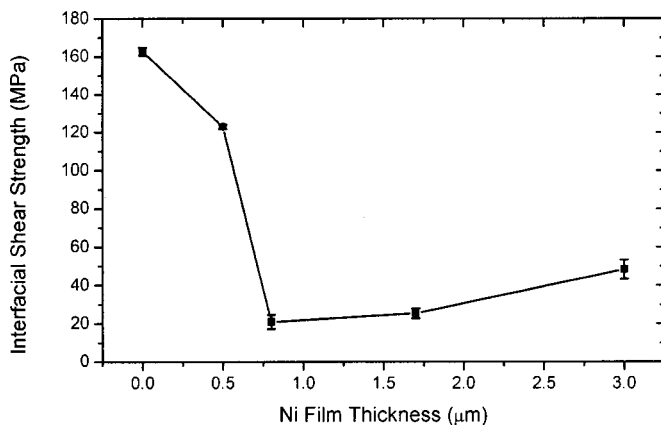


Figure 6. Interfacial shear strengths of SiC_f/7075Al composites containing fibers with different nickel film thicknesses in push-out tests.

facial shear strength slightly increased. With increasing nickel film to 3.0 μm, much less Ni₂Al₃ formed and nickel film was partly retained on the surfaces of the fibers as shown in Fig. 9d, and thus the interfacial shear strength was larger than those of the composites with nickel films of 0.8 and 1.7 μm thick.

Stress-displacement curves.—Figure 10 shows the interfacial shear stress-displacement curves of SiC_f/7075Al composites containing fibers with different nickel film thickness in push-out tests, and Fig. 11 shows the interfacial shear stress drop (τ_d) of these composites. The stress drop τ_d was obtained from the equation

$$\tau_d = S_{p1} - S_{p2} \quad [3]$$

where S_{p1} and S_{p2} are the first peak and first lower point, respectively, as shown in Fig. 10. The τ_d of the composite containing fibers without coating was 21 MPa. The composite with a nickel film thickness of 0.5 μm exhibited the largest τ_d of 42 MPa because of the breaking of strongest chemical bonding between fiber and matrix as discussed above in addition to the difference between static and kinetic friction forces. The one with a nickel film thickness of 0.8 μm rapidly decreased to 3 MPa due to the porous interface providing little bonding. With increasing coating film thickness, more nickel remained leading to less interfacial porosity and then slightly increased τ_d .

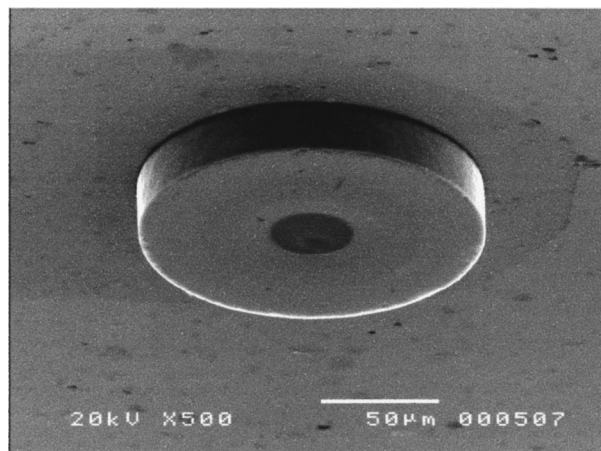
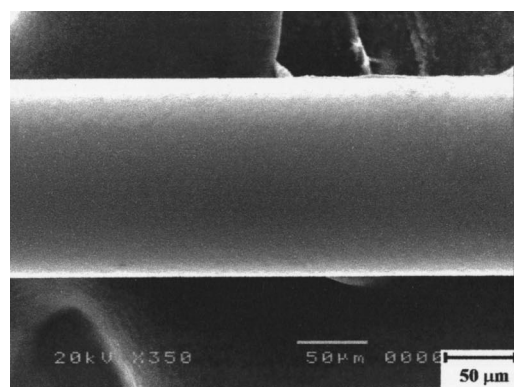
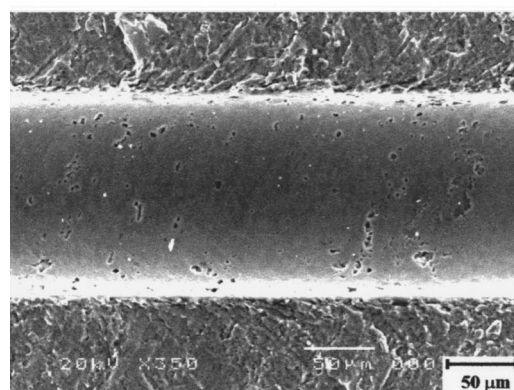


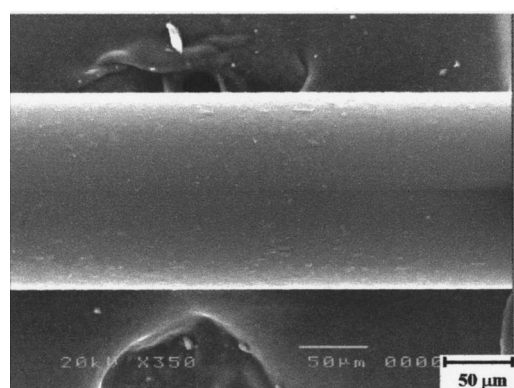
Figure 7. Surface morphology of indented SiC_f/7075Al composite containing fibers without electroless nickel coating.



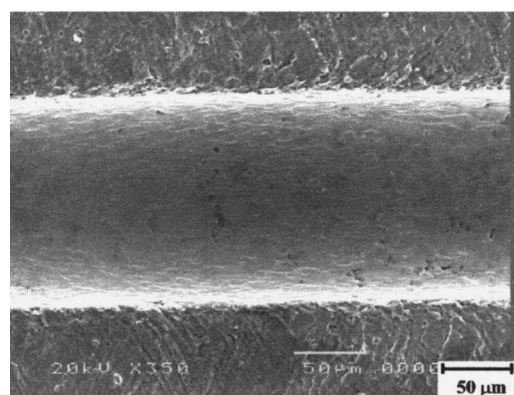
(a)



(b)

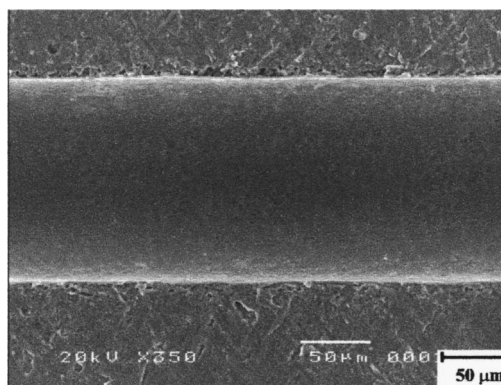


(c)

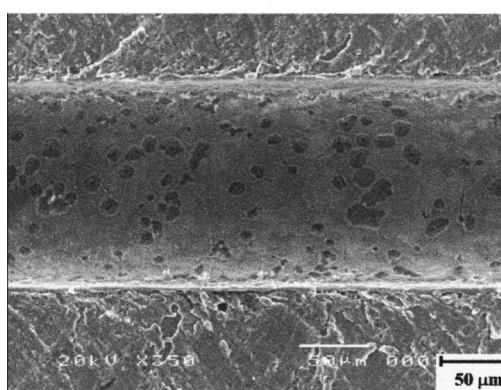


(d)

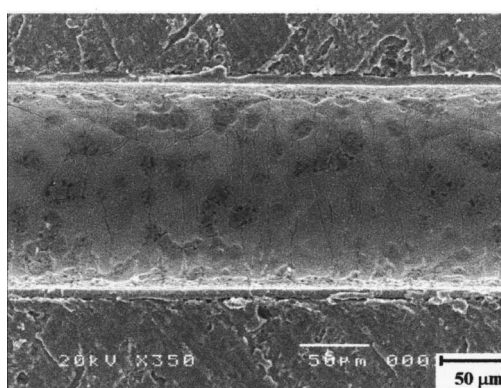
Figure 8. Surface morphologies of (a) SiC fiber and (b) aluminum matrix of the SiC_f/7075Al composite containing fibers without electroless nickel coating before fiber pushed out, (c) SiC fiber and (d) aluminum matrix after fiber pushed out.



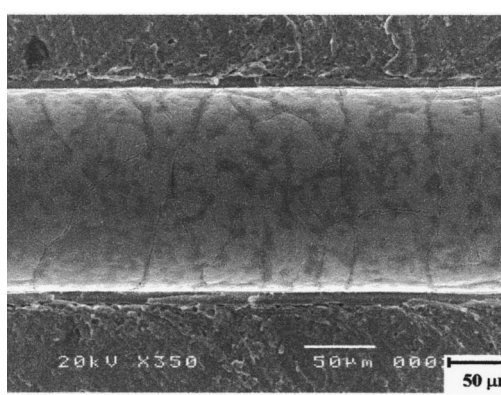
(a)



(b)



(c)



(d)

Figure 9. Surface morphologies of the matrices of SiC_f/7075Al composites containing fibers with electroless nickel coatings of (a) 0.5, (b) 0.8, (c) 1.7, and (d) 3.0 μm thick after fiber push out.

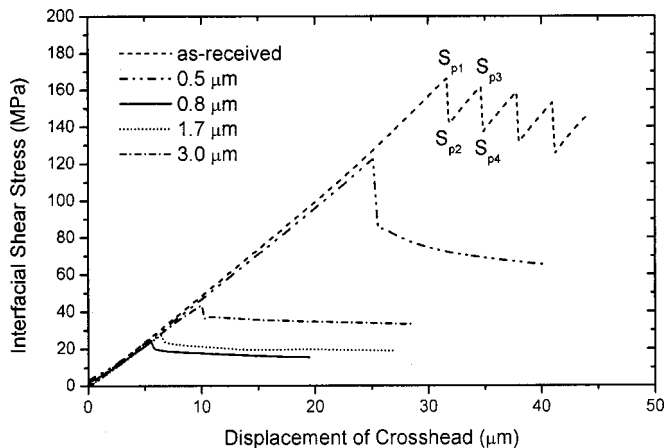


Figure 10. Interfacial shear stress-displacement curves of SiC_f/7075Al composites containing fibers with different nickel film thicknesses in push-out tests.

Fibers without nickel coating.—With increasing crosshead displacement, the interfacial shear stress linearly increased at an elastic stage as shown in Fig. 10. No interfacial decohesion between fiber and matrix occurred until the stress accumulated to first peak S_{p1} (165 MPa). It was proved by Fig. 12, the SEM micrograph of the surface morphology of indented SiC_f/7075Al composite when the indentation was interrupted at the stress of 150 MPa; no interfacial failure was observed. Besides, an α-step meter was used to measure the surface profile of the indented fiber and matrix, and no difference in height between the fiber and the matrix was found when the indentation was stopped at 150 MPa. As the interfacial shear stress increased to the first peak S_{p1}, the interface between fiber and matrix suddenly debonded, and the stress rapidly dropped to a lower point S_{p2} (142 MPa). An obvious displacement of fiber of 5.3 μm was measured by α-step meter within a small displacement of crosshead between S_{p1} and S_{p2} because of the compliance of the test system.¹⁶

Subsequently, with increasing crosshead displacement, the fiber did not move until stress accumulated from S_{p2} to S_{p3} (162 MPa). After that, fiber slid again, and the stress dropped to next low point S_{p4}. This phenomenon cyclically repeated, and the stress fluctuation was as high as 20 MPa. It was realized from Fig. 8c and d that the matrix adjacent to the fibers deformed elastically before the stress accumulated to S_{p1}, followed by obvious fiber sliding and matrix shear after the stress reached S_{p1}. Then a part of the accumulated

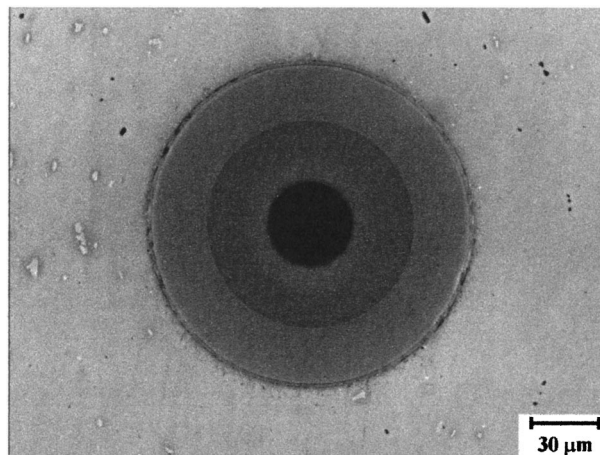


Figure 12. Surface morphology of indented SiC_f/7075Al composite containing fibers without electroless nickel coating when the indentation was interrupted at 150 MPa.

stress released, and the remained stress lowered to S_{p2} and could not drive the fiber to slide. As the crosshead continued to be pushed forward, the stress accumulated to another peak S_{p3}, and then subsequent fiber sliding and matrix shear occurred again. During the stress accumulation and fiber sliding periodicals, the fluctuation amplitude and the displacement almost remained constant. The sliding stress decreased at an average rate of 1.3 MPa/μm, which is much larger than the stress decrease rate of 0.2 MPa/μm caused by the decreasing fiber/matrix interface area due to the trapped matrix debris at the interface reducing the fiber/matrix contact area.

Fibers with nickel coating.—With increasing crosshead displacement, the interfacial shear stresses linearly increased to peaks and then dropped due to the interfacial decohesion as shown in Fig. 10. At the elastic stage, no interfacial decohesion between fiber and matrix occurred until the stresses accumulated to peaks as same as the specimen without nickel coating. However, as the interfaces between the fiber and the matrix suddenly decohered, the stresses rapidly dropped to lower points, and the interfacial shear stresses slowly and smoothly decreased as the third stage. The phenomenon of stress accumulation to second peak never occurred due to the complete failure of interfaces.

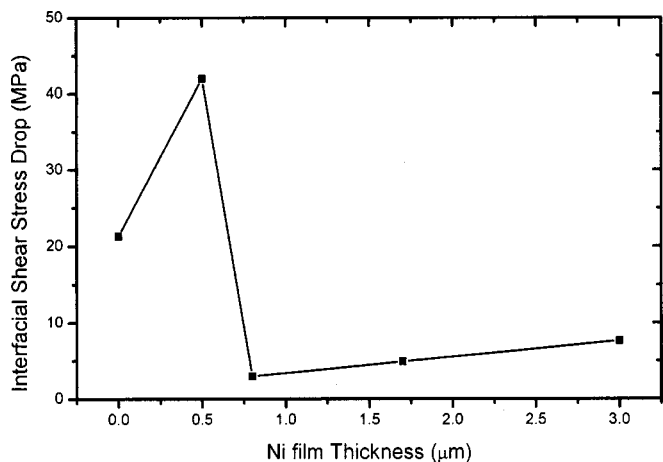


Figure 11. Interfacial shear stress drop (τ_d) of SiC_f/7075Al composites containing fibers with different nickel film thicknesses in push-out tests.

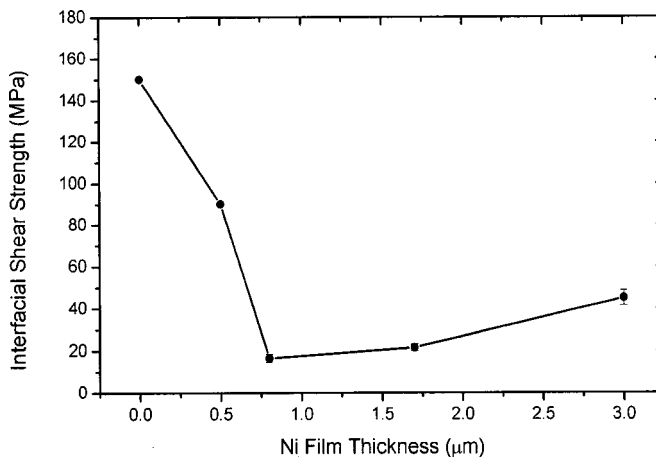


Figure 13. Interfacial shear strengths of SiC_f/7075Al composites containing fibers with different nickel film thickness in push-back tests.

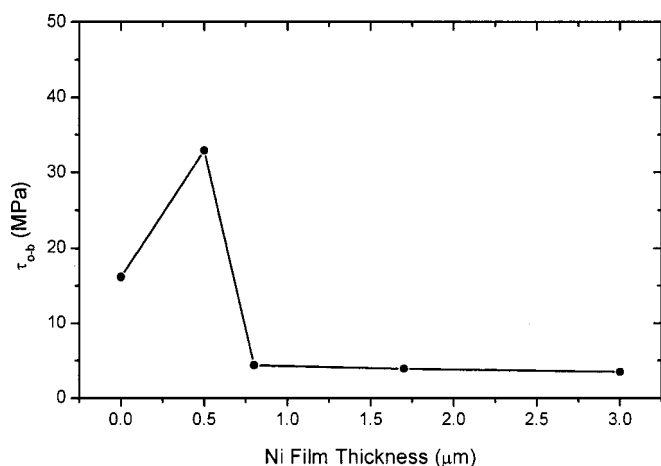


Figure 14. Difference in interfacial shear strengths of composites containing fibers with different nickel film thickness between push out and push-back tests.

The decrease rate of the interfacial shear stress at the third stage was slightly reduced from 0.7 to 0.1 MPa/ μm with increasing nickel film thickness.

Comparison of push-out and push-back tests.— Interfacial shear strengths.—Figure 13 shows the interfacial shear strengths of $\text{SiC}_f/\text{7075Al}$ composites containing fibers with different nickel film thickness in push-back tests. Comparison of the curve shown in Fig. 6, shows that the relationship of strength to film thickness is the same except that the interfacial shear strengths in push-out tests are slightly higher than those in push-back tests.

Figure 14 shows the difference in the interfacial shear strengths between push-out and push-back tests, τ_{ob} , which is mainly attributed to the interfacial chemical bonding. Thus, by comparing Fig. 11, the τ_{ob} of the composites with different nickel film thickness revealed the same trend as τ_d because the breaking of chemical bonding dominated τ_{ob} and τ_d . The τ_{ob} of the composite containing fibers without coating was 16 MPa, and the other composites have the almost same τ_{ob} of about 4 MPa, except the composite with a nickel film thickness of 0.5 μm exhibited the largest τ_{ob} of 33 MPa because of the strongest chemical bonding. The τ_d is larger than τ_{ob} , and the difference between static and kinetic friction force during push-out test contributed the difference between τ_{ob} and τ_d . Exceptionally, the composite with a nickel film thickness of 0.8 μm obviously exhibited an abnormal phenomenon of lower τ_d because of the porous matrix adjacent to fibers. When the fiber was pushed back, the fragment of the fractured porous matrix existed at the interface and increased the difficulty for fiber sliding.

Stress-displacement curves.—Figure 15 shows the interfacial shear stress-displacement curves of $\text{SiC}_f/\text{7075Al}$ composites containing fibers with different nickel film thickness in push-back tests. In the composite containing fibers without coating, an obvious decrease in the amplitude of zigzag was founded with increasing indentation distance because of the abrasion between fiber and matrix. In the composites containing fibers with nickel coating, a stress-drop phenomenon, called “seat drop,” occurred¹⁷ when the fibers were pushed back to its original location before indentation. In the composite without nickel coating, the stress drop was not observed because the original geometry the matrix around interfaces was destroyed when fibers slid during indentation.

Conclusions

The effect of electroless nickel coating on the interfacial shear strengths of silicon carbide continuous fiber reinforced AA 7075

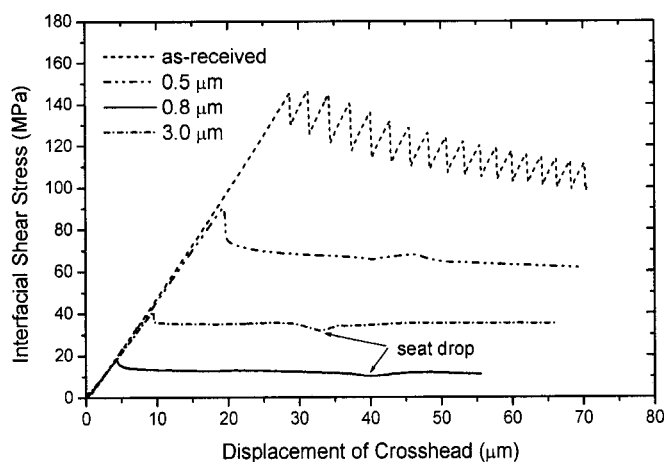


Figure 15. Interfacial shear stress-displacement curves of $\text{SiC}_f/\text{7075Al}$ composites containing fibers with different nickel film thickness in push-back tests.

aluminum matrix composites ($\text{SiC}_f/\text{7075Al}$) was investigated using a push-out method with a WC cone indenter. During indentation, no rupture of fibers was observed. This showed that a push-out test can measure the interfacial shear strength of $\text{SiC}_f/\text{7075Al}$ precisely. The 160 MPa interfacial shear strength of the specimen without coating decreases to 120 MPa for the specimen with 0.5 μm nickel coating, even to 20 MPa with 0.8 μm nickel coating, and then slightly increases with increasing coating film thickness. Nickel film reacted with aluminum matrix to form porous nickel aluminide intermetallic compounds during processing and lower the interfacial shear strength. Stress-displacement curves of the push-out and push-back tests showed a zigzag-type curve after elastic deformation for the $\text{SiC}_f/\text{7075Al}$ composites without coating. However, no zigzag-type curve was found for the nickel coating specimen and a seat drop stress-drop phenomenon was observed for the push-back nickel coating specimen.

Acknowledgments

The authors are pleased to acknowledge the financial support for this research by The National Science Council of Taiwan under grant no. NSC-89-2218-E-007-049. The authors also thank Dr. Shou-Yi Chang for reviewing this manuscript.

National Tsing-Hua University assisted in meeting the publication costs of this article

References

1. S. Mitra, I. Dutta, and R. C. Hansen, *J. Mater. Sci.*, **26**, 6223 (1991).
2. S. Ochiai and Y. Murakami, *J. Mater. Sci.*, **14**, 831 (1979).
3. A. G. Metcalfe, *J. Compos. Mater.*, **1**, 356 (1967).
4. M. C. Watson and T. W. Clyne, *Acta Metall. Mater.*, **40**, 141 (1992).
5. M. K. Brun, *J. Am. Ceram. Soc.*, **75**, 1914 (1992).
6. I. Roman and R. Aharonov, *Acta Metall. Mater.*, **40**, 477 (1992).
7. T. W. Clyne and M. C. Watson, *Compos. Sci. Technol.*, **42**, 25 (1991).
8. H. Y. Liu, L. M. Zhou, and Y. W. Mai, *J. Am. Ceram. Soc.*, **78**, 560 (1995).
9. L. T. Drzal and M. Madhukar, *J. Mater. Sci.*, **28**, 569 (1993).
10. J. A. McElman, *Engineered Materials Handbook Vol 1, Composites*, p. 858, ASM International, Materials Park, OH (1987).
11. C. Y. Yang, S. M. Jeng, and J. M. Yang, *Scr. Metall.*, **24**, 469 (1990).
12. C. Nishimura and C. T. Liu, *Acta Metall. Mater.*, **41**, 113 (1993).
13. D. B. Miracle, *Acta Metall. Mater.*, **41**, 649 (1993).
14. D. K. Shetty, *J. Am. Ceram. Soc.*, **71**, C107 (1998).
15. W. C. Chiou and C. T. Hu, *Metall. Mater. Trans. A*, **25**, 985 (1994).
16. H. Cherouali, G. Fantozzi, P. Reynaud, and D. Roubay, *Mater. Sci. Technol. A*, **250**, 169 (1998).
17. P. D. Jero and R. J. Kerans, *Scr. Metall.*, **31**, 2315 (1990).